Available online at www.sciencedirect.com
ScienceDirect
Journal of Non-Crystalline Solids 353 (2007) 398–404
JOURNAL OF NON-CRYSTALLINE SOLIDS
www.elsevier.com/locate/jnoncrysol

Study on the device characteristics of FePc and FePcCl organic thin film Schottky diodes: Influence of oxygen and post deposition annealing

K.R. Rajesh *, C.S. Menon

School of Pure and Applied Physics, Mahatma Gandhi University, Kottayam 686560, Kerala, India

Received 26 February 2006; received in revised form 21 October 2006
Available online 31 January 2007

Abstract

Device characteristics of Al/FePc/Au and Al/FePcCl/Au are performed and found to show rectification properties. The basic diode parameters of the device are determined. The electrical conductivity has been measured both after exposure to oxygen for 20 days and after annealing at temperature up to 473 K. Current density–voltage characteristics under forward bias are found to be due to ohmic conduction at lower voltage regions. At higher voltage regions there is space charge limited conductivity (SCLC) controlled by a discrete trapping level above the valance edge. The electrical parameters of oxygen doped and annealed samples in the ohmic and SCLC region are determined. The reverse bias curves are interpreted in terms of a transition from electrode-limited Schottky emission to the bulk-limited the Poole–Frenkel effect. The Schottky barrier parameters of oxygen doped and annealed structures of FePc and FePcCl are determined from the C^2–V characteristics.

PACS: 72.80.Le; 73.40.Rw; 73.40.−c; 73.30.+y

Keywords: Devices; Conductivity; Vapor phase deposition; Polymers and organics; Surfaces and interfaces

1. Introduction

During the past fifteen years dramatic advances have been achieved in the performance of organic semiconductor devices. Organic light emitting diodes, for example, were first demonstrated in the late '80s and can already be found in cell phone displays. Attractive features of these materials are the possibility of device processing, compatibility with flexible substrates, and the low materials consumption for ultrathin molecular films, all of which offer the prospect of cheaper photovoltaic energy generation. Large-scale production is easier than for inorganic materials. The greatest peculiarity of organic material is that they can be tuned chemically, in order to adjust separately the band gap, valence and conduction band energies, charge transport, as well as the solubility or other structural properties. Phthalocyanines (Pc) are a class of highly stable organic compounds, which are classified as p-type semiconductor characterized by low mobility and low carrier concentration [1]. The conductivity of these materials depends on the gaseous environment, and thus gas sensors based on phthalocyanines have recently attracted considerable interest [2]. Oxygen is found to have a very large influence on the photovoltaic behavior of Pc-based junctions [3]. Oxygen creates acceptor levels with in the band gap of these materials. Oxygen can act as an ionization center in the phthalocyanine lattice according to the expression

$$\mathrm{MPc} + \mathrm{O_2} \leftrightarrow \mathrm{MPc}^{\oplus} + \mathrm{O}_2^{\ominus} \leftrightarrow h^{\oplus} + \mathrm{MPc} + \mathrm{O}_2^{\ominus}$$

where MPc is the metal-substituted phthalocyanine and $h^{\oplus}$ is a hole. Therefore it can favor the charge separation process upon the thermal degradation of the electronic excitation. Relatively few studies have conducted on iron phthalocyanine chloride (FePcCl) thin films. The object of this paper is to study the electrical conductivity of FePc

* Corresponding author. Tel.: +91 94472 89696.
E-mail address: rajthinfilms@yahoo.co.in (K.R. Rajesh).

0022-3093/$ - see front matter © 2006 Elsevier B.V. All rights reserved.
doi:10.1016/j.jnoncrysol.2006.12.016

and FePcCl sandwich structures using ohmic gold [4,5] and blocking aluminium [6] electrodes. The effects of oxygen doping and annealing on the conductivity properties are also investigated. These studies are capable of providing considerable insight into the charge transport mechanisms and carrier trapping in this material, and such information is of particular importance in the development of viable thin film gas sensing devices.

2. Experimental details

The FePc and FePcCl powder obtained from Aldrich Inc. USA are used as the source material. Sandwich samples are prepared by thermal evaporation at a base pressure of 10^{-5} Pa. Pre-cleaned glass plates coated with evaporated gold electrode, are used as the substrates. The thickness of the films are measured using the Tolansky's multiple beam interference technique with in the error limit ± 1 nm [7]. The thickness of the samples are in the range 400–675 nm. The rates of deposition are typically 0.5 nms^{-1}. The area of each sample studied is 1.2×10^{-5} m^2. Before evaporating the top aluminium electrode one film is kept exposed to dry air for 20 days and another annealed in air at 473 K for 3 h in a furnace attached to a programmable temperature controller. The schematic of the device is shown in Fig. 1. Sample currents are measured using a stabilized power supply and a Keithley electrometer (model no. 617). The temperature is measured using a Cr–Al thermocouple placed in close proximity to the specimen. Capacitance measurements performed using a Hioki 3532 LCR Hi-tester. To avoid contamination, measurements are performed in a subsidiary vacuum of 10^{-3} Pa. The samples are shielded from incident light to avoid photoelectric effect.

3. Results

Fig. 2 shows the typical I–V characteristics of Al/FePc/Au and Al/FePcCl/Au structures. The forward bias direction corresponds to the situation when the bottom gold electrode is positive. The space charge region is detected in the I–V plots by giving rise to a rectification effect. The rectifying behavior of a Schottky barrier diode is assumed to follow a standard thermionic emission theory for conduction across the junction. Based on this theory the current voltage relationship can be expressed [8] as

$$J = J_0(\exp(eV/nkT) - 1) \quad (1)$$

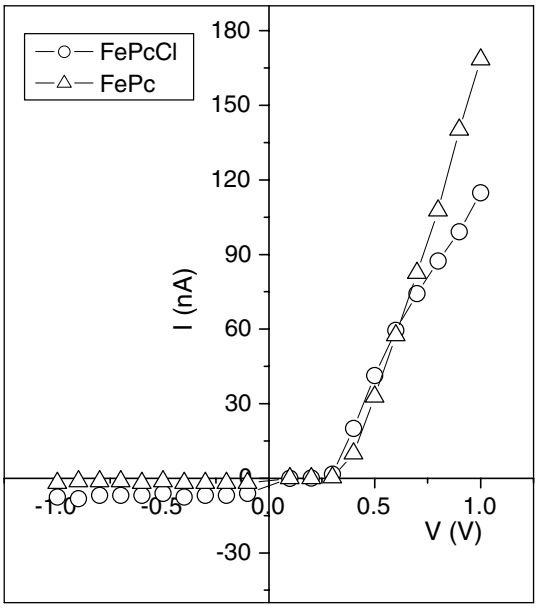

Fig. 2. I–V characteristics of the Al/FePc/Au and Al/FePcCl/Au.

where J is the instantaneous current density, J_0 is the saturation current density, e is the electronic charge, V is the applied potential, n is a constant called diode ideality factor, k is the Boltzman constant and T the absolute temperature. Since $eV/nkT \gg 1$ a semi logarithmic plot of current density versus applied voltage is expected to be linear with a Y intercept corresponding to J_0. Fig. 3 shows the ln$J$

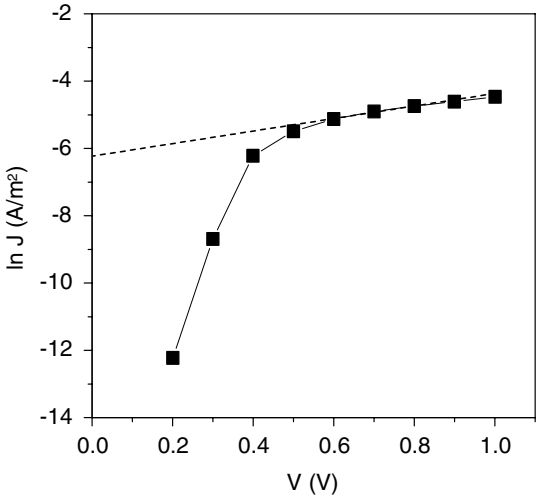

Fig. 3. ln$J$ versus V for FePcCl.

Fig. 1. Schematic of the Al/Pc/Au device.

versus V plot for the Au/FePcCl/Al diode. From the slope value of n is calculated. Table 1 gives the basic diode parameters of FePc and FePcCl. Fig. 4 shows the dependence of capacitance C on the reciprocal film thickness, $1/d$ for FePcCl. Here the capacitance measurements are made at 1 KHz. The linearity of the plot can be analyzed in terms of the capacitance of a parallel plate capacitor

$$C = \varepsilon A/d \tag{2}$$

where ε is the permittivity of phthalocyanine layer, A is the area (1.2×10^{-5} m^2) and d is the thickness of the sample.

Wide-ranging information about the transport mechanism through the phthalocyanine film can be obtained from the analysis of current density (J) – voltage (V) characteristics. The forward J–V characteristics of oxygen doped and annealed Al/FePc/Au structures are shown in Fig. 5. The plots of ln$J$ versus ln$V$ for the oxygen doped and annealed Al/FePcCl/Au are shown in Fig. 6. In these J–V characteristics, two distinct regions can be identified. At low voltages, the slope of ln$J$ versus ln$V$ plot is approximately unity. These plots suggest ohmic conduction at low voltages. Assuming conduction is via holes, the current flow may be expressed in the form [9]

$$J = ep_0\mu_p(V/d) \tag{3}$$

where p_0 is the concentration of thermally generated holes in the valance band, e is the electronic charge, μ_p is the hole

Table 1
Diode parameters of FePc and FePcCl devices

	Saturation current density J_0 (A/m^2)	Diode ideality factor (n)
Au/FePc/Al	1.23×10^3	2.09
Au/FePcCl/Al	1.93×10^3	2.11

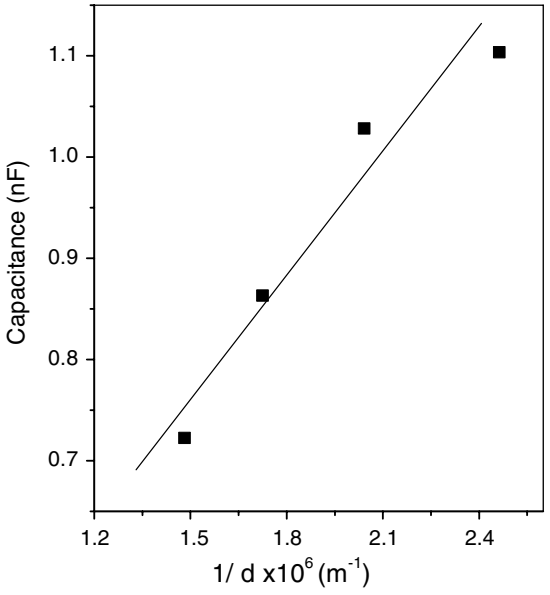

Fig. 4. Capacitance versus $1/d$ for FePcCl.

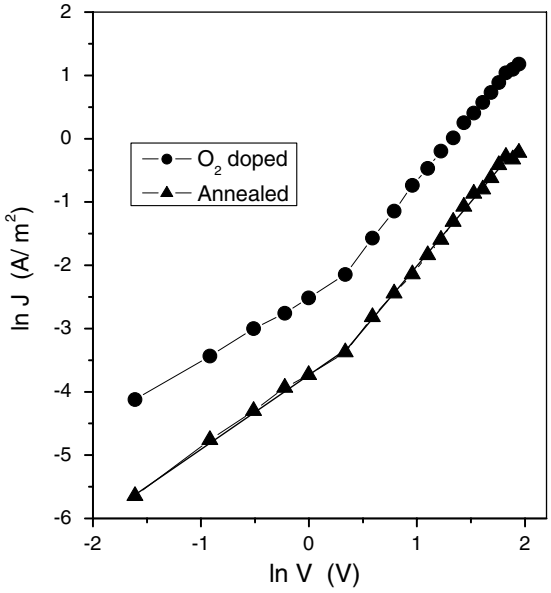

Fig. 5. ln$J$ versus ln$V$ for Al/FePc/Au.

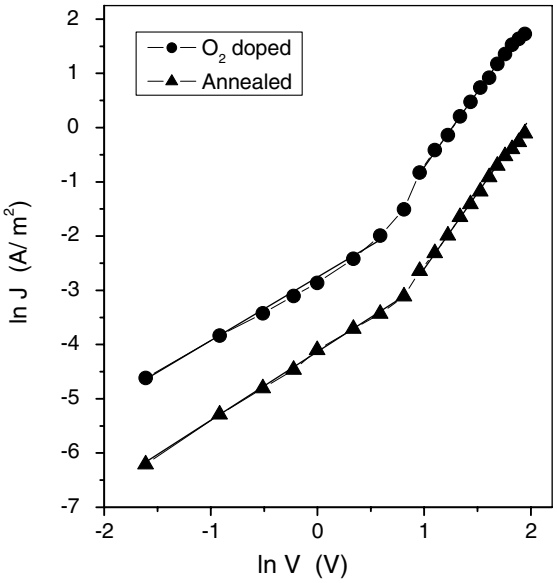

Fig. 6. ln$J$ versus ln$V$ for Al/FePcCl/Au.

mobility and d is the thickness of the film. The concentration of holes at thermal equilibrium is given by

$$p_0 = N_v \exp[-(E_f - E_v)/kT] \tag{4}$$

where N_v is the effective density of state in the valance band, $(E_f - E_v)$ is the separation of Fermi level from the valence band edge, k is the Boltzmann constant and T is the absolute temperature. Now with Eq. (3), the current density in the ohmic region becomes

$$J = e\mu_p N_v (V/d) \exp[-(E_f - E_v)/kT] \tag{5}$$

By plotting ln(J/V) against $1000/T$ (Fig. 7), the values of $(E_f - E_v)$ and μ_p N_v have been calculated from the slope

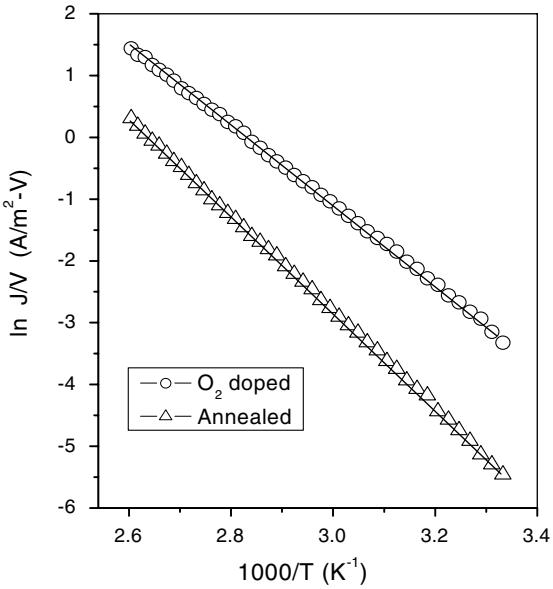

Fig. 7. Typical plot of $\ln(J/V)$ versus $1000/T$ for Al/FePc/Au.

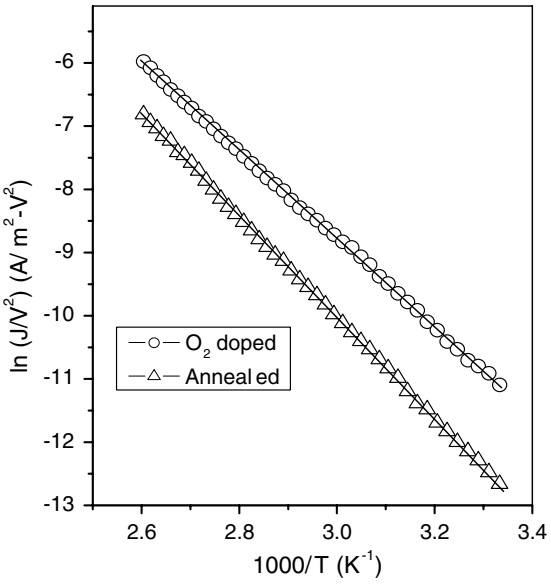

Fig. 8. $\ln(J/V^2)$ versus $1000/T$ for Al/FePcCl/Au.

and intercept at $1/T = 0$. Taking $N_v = 10^{27}$ m^{-3} which correspond to one state per molecule [10], the values of $(E_f - E_v)$, μ_p and p_0 are calculated for FePc and FePcCl and are tabulated in Table 2.

In the higher voltage regime of the J–V characteristics (Figs. 5 and 6), the slope of $\ln J$ versus $\ln V$ plot is approximately equal to 2, which shows that current is SCLC controlled by the relationship [10]

$$J = (9/8)\varepsilon\mu_p\theta(V^2/d^3) \tag{6}$$

where ε is the permittivity of the layer and θ is the ratio of free to trapped charge carrier density or trapping factor given by [10]

$$\theta = (N_v/N_t)\exp[-(E_t - E_v)/kT] \tag{7}$$

where N_t is the total trap concentration at the energy level, $E_t - E_v$ is the activation energy of hole traps, k is the Boltzmann constant and T is the absolute temperature. Using the above expression current density in the SCLC becomes

$$J = (9/8)\varepsilon\mu_p(N_v/N_t)(V^2/d^3)\exp[-(E_t - E_v)/kT] \tag{8}$$

From the above expression it is evident that $\ln(J/V^2)$ versus $1000/T$ should be a straight line. The slope and intercept at $1/T = 0$ on the current axis give $E_t - E_v$ and N_t, respectively. $E_t - E_v$ and N_t, are determined from the $\ln(J/V^2)$ versus $1000/T$ plots. Fig. 8 shows $\ln(J/V^2)$ versus $1000/T$ for the oxygen doped and annealed FePcCl thin films.

Table 2
Variation of electrical parameters in ohmic region

Sample	$E_f - E_v$ (eV)	μ_p (m^2 V^{-1} s^{-1})	p_0 (m^{-3})
Oxygen doped FePc	0.55 ± 0.02	3.82×10^{-6}	3.9×10^{18}
Annealed FePc	0.67 ± 0.02	2.87×10^{-6}	4.5×10^{18}
Oxygen doped FePcCl	0.64 ± 0.02	3.38×10^{-6}	5.2×10^{18}
Annealed FePcCl	0.69 ± 0.02	2.72×10^{-6}	5.3×10^{18}

Table 3
Variation of electrical parameters SCLC region

Sample	$E_t - E_v$ (eV)	N_t (m^{-3})	θ
Oxygen doped FePc	0.68 ± 0.02	3.18×10^{21}	1.21×10^{-6}
Annealed FePc	0.73 ± 0.02	4.51×10^{21}	1.24×10^{-7}
Oxygen doped FePcCl	0.60 ± 0.02	4.18×10^{23}	2.03×10^{-7}
Annealed FePcCl	0.69 ± 0.02	4.62×10^{23}	7.66×10^{-9}

Using these values in Eq. (7) the trapping factor θ is estimated. The obtained values of $E_t - E_v$, N_t and θ are given in Table 3.

The depletion layer or space charge capacitance associated with a p-n junction or Schottky barrier is given by [11]

$$1/C^2 = 2[V_{bi} - V - (kT/e)]/e\varepsilon NA^2 \tag{9}$$

where N is the effective density of donor and acceptor, A is the area, e is the electronic charge, V is the applied voltage and V_{bi} is the barrier height. Fig. 9 shows the variation of $1/C^2$ with V for oxygen doped and annealed structures of FePcCl. It is clear that $1/C^2$ versus V plots gives N [12].

The barrier height of Schottky diode ϕ, is related to the diffusion potential, V_{bi}, by the following Eq.

$$\phi = V_b + kT/e[1 + \ln(N_v/N)] \tag{10}$$

and depletion layer width (W) is given by

$$W = (2\varepsilon V_{bi}/eN)^{1/2} \tag{11}$$

The capacitance C_0, at zero bias which associated with the depletion width W of high resistance, is determined for both oxygen doped and annealed structures [13]. In addition, the maximum electric field attainable in the depletion layer could be calculated from the relation

$$E_{max} = 2V_{bi}/W \tag{12}$$

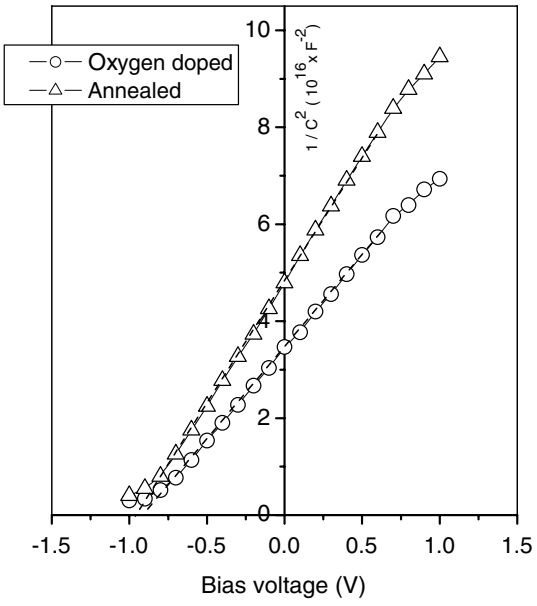

Fig. 9. Variation of $1/C^2$ with V for FePcCl.

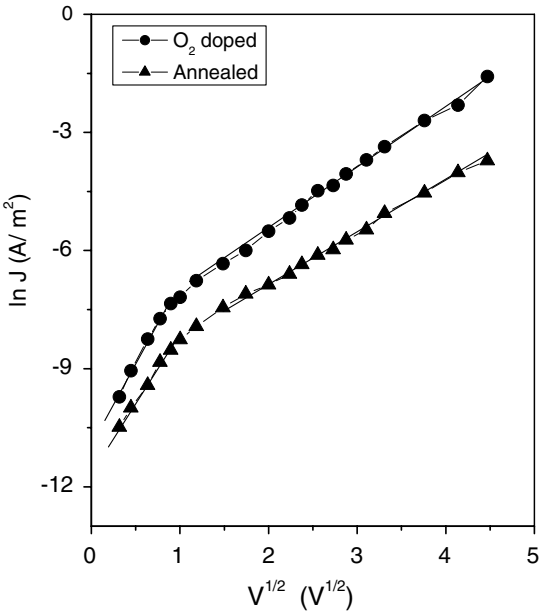

Fig. 10. Reverse bias $\ln J$–$\ln V^{1/2}$ characteristics for FePc at 300 K.

The values of space charge density N, built-in potential or diffusion potential V_{bi}, depletion width W, barrier height ϕ, zero bias capacitance C_0 and maximum electric field E_{max} for FePc and FePcCl are listed in Table 4.

The reverse bias current–voltage characteristics also give information about the properties of metal-semiconductor contact. Figs. 10 and 11 show the reverse bias $\ln J$ versus $\ln V^{1/2}$ for FePc and FePcCl at room temperature, which clearly yield two distinct regions.

For Schottky emission the current density J is expressed as follows [14,15],

$$J = A^* T^2 \exp(-\phi/kT) \exp(e\beta_s V^{1/2}/kTd^{1/2}) \tag{13}$$

where A^* is the effective Richardson constant, ϕ is the Schottky barrier height at the injected electrode and β_s is the Schottky field lowering constant. For Pool–Frenkel emission, the current density is given by

$$J = J_{pfo} \exp(\beta_{pf} V^{1/2} q/kTd^{1/2}) \tag{14}$$

where β_{pf} is the Pool–Frenkel coefficient. The theoretical values of these coefficients are given by

$$2\beta_s = \beta_{pf} = (e/\pi\varepsilon)^{1/2} \tag{15}$$

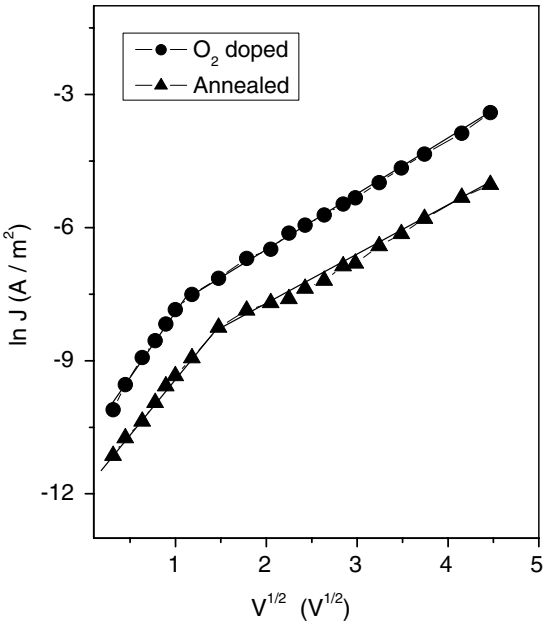

Fig. 11. Reverse bias $\ln J$–$\ln V^{1/2}$ characteristics for FePcCl at 300 K.

The theoretical values β_s and β_{pf} of are found to be 2.08×10^{-5} and 4.17×10^{-5} in $eV/\sqrt{(Vm^{-1})}$ for FePc and 1.77×10^{-5} and 3.54×10^{-5} for the FePcCl samples.

Table 4
Variation of Schottky depletion layer parameters

Sample	N (m^{-3})	V_{bi} (eV)	W (nm)	ϕ (eV)	E_{max} (eV/μm)	C_0 (nF)
Oxygen doped FePc	8.99×10^{22}	0.82	57.6	1.14	27.42	6.03
Annealed FePc	6.76×10^{22}	0.86	68.1	1.19	25.24	5.22
Oxygen doped FePcCl	5.60×10^{22}	0.91	90.8	1.24	20.03	5.39
Annealed FePcCl	4.10×10^{22}	0.94	107.9	1.28	17.42	4.56

Error bar for V_{bi}, W and ϕ are ±0.02 eV, ±0.1 nm and ±0.02 eV, respectively.

4. Discussion

The rectification effect observed in the I–V plot can be explained by the low work function of Al and high work function of Au and by the p-type conduction of FePc and FePcCl. This is attributed to the blocking contact or a Schottky barrier which is formed at the Al/FePc and Al/FePcCl interfaces, where the conduction and valence band edges bend downward at equilibrium. The Au electrode having a high work function, $\phi = 5.47$ [16] forms an ohmic contact with the phthalocyanine layer. It is clear from Fig. 3 that a linear relationship exists for small-applied voltages and for large-applied voltages the graph deviates from linearity. The voltage drop across the series resistance in the natural region of the semiconductor causes this deviation. The value of ε is estimated from Fig. 4 and found to be 4.064×10^{-11} Fm^{-1}. From a similar procedure the value ε of is determined to be 2.92×10^{-11} Fm^{-1} for FePc. The above-derived values of permittivity are in good agreement with the values in the range of 2.12–4.5×10^{-11} Fm^{-1} for CuPc and PbPc [17–19].

The main feature of Figs. 5 and 6 are that the current density of O_2 doped samples is significantly higher than those for the annealed samples. This lowering indicated that the annealing process has resulted in the removal of considerable quantities of oxygen acceptor impurities [3,20]. The values of $(E_f - E_v)$, μ_p and p_0 given in Table 2. suggest that FePc and FePcCl are p-type organic semiconductors with low mobility and relatively high thermal activation energy. From Table 3 it can be seen that the trapping energy $E_t - E_v$ increases when the samples are annealed in air. This may be due to an intrinsic activation process, which probably results from the removal of impurities during annealing process [5].

According to Beth's model [13], which is commonly used when a thin insulating layer separates the semiconductor from the barrier electrode, the intercept of $1/C^2$ versus V plot (Fig. 8) with the horizontal asymptote, rather than the base line, leads to the value of V_{bi} as given by Eq. (9). However, the space charge in the depletion region results from doping of phthalocyanine layer by oxygen and presumably exists as ionized oxygen. It is clear from Table 4 that the values of N for oxygen doped samples are higher than those for the annealed samples. The higher field E_{max}, for these samples may be responsible for their high carrier concentration. It is evident that the solution to improve the performance of phthalocyanine sensing devices is to increase the acceptor concentration and to decrease the trap density. Thus oxygen is found to have a profound influence on the device characteristics of phthalocyanine based junctions.

The reverse current arises due to recombination of charge carriers, release of charge carriers from trap levels, barrier lowering at high electric field or leakage. The linear sections of the curves (Figs. 10 and 11) can be interpreted in terms of either the Schottky emission or Pool–Frenkel emission. The values of β calculated from the slopes of the low voltage regions of Fig. 10 are found to be 7.21×10^{-5} and 6.0×10^{-5} for oxygen doped and annealed FePc, respectively. For FePcCl samples (Fig. 11), values of β are 5.8×10^{-5} and 4.64×10^{-5}, respectively. These values differ from both the expected Schottky and Pool–Frenkel values. Similar behavior has been reported previously for phthalocyanine films using aluminium-injected electrodes [5,14,15,21] and is interpreted in terms of the Schottky depletion region of thickness W. Putting the theoretical value of β_s for FePc into Eq. (9), for oxygen doped samples the values of $W = 58.2$ nm and $\phi = 1.02$ eV and for annealed samples $W = 69.7$ nm and $\phi = 1.1$ eV have been obtained. Following a similar procedure yield, $W = 91.9$ nm and $\phi = 1.19$ eV for oxygen doped FePcCl and $W = 117$ nm and $\phi = 1.23$ eV for the annealed FePcCl. These values are found close to the values calculated from the $C^2 - V$ characteristics. These results suggest that in the low field region the conduction mechanism is controlled by Schottky emission over the space charge region formed at the metal/organic semiconductor interface. At low field conduction by Schottky emission is reported in the case of ZnPc device [22].

The values of β for FePc derived from the slopes of the high voltage sections of Fig. 10 are found to be 3.88×10^{-5} and 3.37×10^{-5} for oxygen doped and annealed samples, respectively. In the case of FePcCl (Fig. 11) these values are 3.17×10^{-5} and 3.04×10^{-5}, respectively. In the higher voltage region experimental values of β for annealed samples is in close agreement with the theoretically calculated values of β_{pf}, suggesting that the conduction is bulk-limited in this range. Thus it appears that the effect of annealing may improve the uniformity of electric field distribution in FePc and FePcCl thin films.

5. Conclusion

Current density–voltage measurements on Al/FePc/Au and Al/FePcCl/Au structures for both oxygen doped and annealed samples show characteristics of typical Schottky-barrier devices. From the dependence of capacitance C on the reciprocal film thickness the permittivity of the samples are calculated. Under forward bias, two separate regions are observed. These characteristics show ohmic conductivity at low voltages and space charge limited conductivity at higher voltages. The electrical parameters of oxygen doped and annealed samples in the ohmic and SCLC region are determined. The reverse bias curves are interpreted in terms of an electrode-limited to bulk-limited transition from Schottky emission to the Poole–Frenkel effect. Information on the thickness of the depletion region, diffusion potential, barrier height, and acceptor density of holes, can be successfully obtained by analyzing the characteristics for both oxygen doped and annealing samples. It can be concluded from these measurements that, oxygen have a large influence on the parameter values of W, ϕ and N. In general, the present results put the accent on the role of oxygen doping and the existence of interfacial

oxide layer in the determination of the electrical characteristics of FePc and FePcCl based devices.

References

[1] R.D. Gould, Coord. Chem. Rev. 156 (1996) 237.
[2] R.A. Collins, K.A. Mohammed, J. Phys. D 21 (1998) 154.
[3] T.G. Abdel-Malik, Thin Solid Films 205 (1991) 241.
[4] T.G. Abdel-Malik, A.A. Ahmed, A.S. Riad, Phys. Status Solidi (a) 121 (1990) 507.
[5] S. Gravano, A.K. Hassan, R.D. Gould, Int. J. Electron. 70 (1991) 477.
[6] M. Martin, J.J. André, J. Simon, Nouv. J. Chim. 5 (1981) 485.
[7] L.I. Maissel, R. Glang, Hand Book of Thin Film Technology, Mc Graw-Hill, New York, 1983.
[8] S.M. Sze, Physics of Semiconductor Devices, Eastern Wiley, New Delhi, 1981.
[9] Y. Sadaoka, T.A. Jones, W. Gopel, J. Mater. Sci. Lett. 8 (1989) 1095.
[10] A.K. Hassan, R.D. Gould, Int. J. Electron. 74 (1993) 59.
[11] E.H. Rhoderick, R.H. Williams, Metal-Semiconductor Contacts, 2nd Ed., Clarendon, Oxford, 1988.
[12] A.K. Ghosh, T. Feng, J. Appl. Phys. 44 (1973) 2781.
[13] A.S. Riad, S.M. Khalil, S. Darwish, Thin Solid Films 249 (1994) 219.
[14] W. Wilson, R.A. Collins, Sens. Actuat. 12 (1978) 389.
[15] G.D. Sharma, Synth. Metals 74 (1995) 227.
[16] M. Michel, J.J. André, J. Simon, J. Appl. Phys. 54 (5) (1983) 2792.
[17] A. Ahamed, R.A. Collins, Phys. Status Solidi (a) 123 (1991) 201.
[18] R.D. Gould, Thin Solid Films 125 (1985) 63.
[19] R.D. Gould, J. Phys. D: Appl. Phys. 9 (1986) 1785.
[20] A.J. Twarowski, J. Chem. Phys. 77 (1982) 5840.
[21] J.G. Simmons, J. Phys. D. 38 (1971) 2378.
[22] F.R. Fan, L.R. Faulkner, J. Chem. Phys. 69 (1978) 3334.